Contribution Analysis of GOCE SGG Observations at Different Orbital Altitudes to Tongji-GMMG2021S Gravity Field Model

Jianhua Chen, Qiujie Chen [iD], Yunzhong Shen [iD], and Xingfu Zhang

Abstract—**Gravity field and steady-state ocean circulation explorer (GOCE) satellite gravity gradiometry (SGG) data play an important role in modeling static gravity fields, particularly considering the decrease in orbital altitude from 259.5 to 229.0 km during the final 15 months. However, there is limited discussion regarding the contribution of decreases in the GOCE satellite's orbital altitude to the static gravity field solutions. Therefore, by utilizing reprocessed Level-1B SGG data and gravity recovery and climate experiment (GRACE) satellite data, we have solved a satellite-only static gravity field model entitled Tongji-GMMG2021S up to 300 d/o. Subsequently, a quantitative analysis was conducted to assess the contribution of SGG data during the period of low-orbital altitude (LOA) from August 2012 to October 2013 towards the Tongji-GMMG2021S solution. The validation results indicated that the accuracy of the Tongji-GMMG2021S model was comparable to that of the latest combined GOCE/GRACE models. During the LOA period, the analysis conducted at the normal matrix level demonstrated that the SGG data obtained during the LOA period significantly contributed to the solutions at medium and high degrees. Notably, the final 5-month SGG data contributed more than 25% to the Tongji-GMMG2021S solution within the range of 150 to 260 d/o. Furthermore, beyond 180 degrees, the contribution of the solution for the LOA period was even more significant than that for the high-orbital altitude (HOA) period from November 2009 to July 2012. The LOA solution exhibited a standard deviation of 7.24 cm in geoid height error with respect to Tongji-GMMG2021S, resulting in a reduction of 51.15% in standard deviation compared to the HOA solution (14.82 cm).**

Index Terms—**Contribution analysis, gravity field and steady-state ocean circulation explorer (GOCE), gravity field estimation, orbital altitude, satellite gravity gradiometry (SGG).**

I. INTRODUCTION

THE Earth's gravity field is a fundamental physical field that objectively exists within the Earth, reflecting the spatial distribution of surface mass and the density of internal mass, as well as temporal variations in mass transport [1], [2], [3]. It plays a crucial role in determining geoid height [4] and monitoring variations in terrestrial water storage [5]. The gravity field and steady-state ocean circulation explorer (GOCE) mission, developed by the European Space Agency (ESA) was successfully launched in March 2009 and operated close to a sun-synchronous orbit, maintaining an orbital inclination of 96.7° [6]. It is the first gravity mission equipped with an electrostatic gravity gradiometer (EGG) for observing the second-order derivative of the gravitational potential. One of its objectives is to provide a high-resolution and high-precision static gravity field model with a geoid accuracy of 1–2 cm and a gravity anomaly accuracy of approximately 1 mGal (1 mGal = 10^{-5} m/s^2) at a spatial resolution of 100 km (corresponding to spherical harmonic coefficients up to degree and order [d/o] 200) [7].

The GOCE high-level processing facility (HPF) continuously updates the GOCE satellite dataset since its initial release, intending to enhance its quality. Currently, six generations of GOCE gravity field models have been published, primarily involving direct, time-wise, and space-wise approaches. One of the significant differences between the first and fifth generations of GOCE gravity field solutions is the gradual increase in data volume and improvement in spatial resolution. The sixth generation distinguishes itself from the fifth generation by incorporating the latest release of satellite gravity gradiometry (SGG) data, resulting in a further enhancement in model accuracy. The reprocessed SGG data exhibits a significant reduction in low-frequency noise compared to the previous SGG dataset [8]. Several static gravity field models have been developed using different strategies based on this dataset and published on the International Centre for Global Earth Models (ICGEM).[1] The GO_CONS_GCF_2_DIR_R6 model completes up to 300 d/o was derived from the GOCE SGG, gravity recovery and climate experiment (GRACE), and satellite laser ranging (SLR) observations using the direct approach [9]. Combining GOCE (normal equation of GO_CONS_GCF_2_TIM_R6), GRACE (normal equation of ITSG-Grace2018s), low-Earth orbiter kinematic orbits, and SLR observations, the satellite-only gravity field model GOCO06s was determined from the Gravity Observation Combination project [10]. Tongji gravity field model from

Jianhua Chen, Qiujie Chen, and Yunzhong Shen are with the College of Surveying and Geo-informatics, Tongji University, Shanghai 200092, China (e-mail: jianhuachen@tongji.edu.cn; qiujiechen@tongji.edu.cn; yzshen@tongji.edu.cn).

Xingfu Zhang is with the Departments of Surveying and Mapping, Guangdong University of Technology, Guangdong 510006, China (e-mail: xfzhang 77@163.com).

[1][Online]. Available: http://icgem.gfz-potsdam.de/tom_longtime, last access: 30 April 2024.

multigravity observations [**S**atellites] (Tongji-GMMG2021S) is a combined GOCE/GRACE model developed by Tongji University that integrates GOCE SGG data and GRACE data at the normal equation level through a direct approach [11]. Based on the GOCE SGG data, GOCE kinematic orbits, and GRACE normal equation provided by Southwest Petroleum University, Wuhan University constructed the WHU-SWPU-GOGR2022S model [12]. In addition, static gravity field models are exclusively derived from GOCE satellite data or generated by integrating ground gravity data. For more information, please refer to the literature [13], [14], [15].

However, the accuracy and spatial resolution of the gravity field models are constrained by various factors, including but not limited to the diversity of observation types, data spans, observation accuracies, data sampling rates, and orbital altitudes [10], [13], [16], [17], [18], [19]. Farahani et al. [17], Yi et al. [20], and Bruinsma et al. [21] provided detailed discussions on the contributions of various types of data to static gravity field models, including the kinematic orbit and SGG data from the GOCE satellite. In the combined model, Kvas et al. [10] only quantitatively analyzed the different types of observations for the static gravity field model. According to the gravitational potential formula, a decrease in the orbital altitude is likely to result in increased sensitivity of SGG data for gravity field modeling. However, there is limited research on the impact of decreased orbital altitude on the accuracy of GOCE static gravity field models. Bruinsma et al. [21], [22] noted distinct contributions from the data collected during the final 14 months of GOCE's scientific mission compared to the preceding 28 months. Wu [19] conducted a study to investigate how the reduction of orbital altitudes of the GOCE satellite affects the accuracy of the GOCE SGG-only static gravity field model in terms of geoid degree variance (GDV) and noise levels in SGG data. However, accurately determining low-degree spherical harmonic coefficients using only SGG data from the GOCE satellite is not feasible. There is a lack of analysis regarding the contribution made by SSG at different orbital altitudes in the combined static gravity field model. In addition, previous studies were based on an outdated release of the SGG dataset, which is susceptible to low-frequency errors. Although Brockmann et al. [13] used a reprocessed SGG dataset to develop the GO_CONS_GCF_2_TIM_R6 model, their study solely examined the impact of different releases of the SGG dataset at two orbital altitudes on the gravity field model, without conducting a quantitative analysis its contributions.

The orbital altitude underwent two distinct phases during the GOCE scientific mission period. The high-orbital altitude (HOA) flight phase occurred at a mean altitude of 259.5 km from November 2009 to July 2012. The low-orbital altitude (LOA) flight phase occurred from August 2012 to October 2013, during which the orbital altitudes decreased from 259.5 km down to 229.0 km. In particular, four significant orbital reduction operations in the LOA period were performed in August 2012, November 2012, February 2013, and May 2013 [23], [24]. From a mathematical perspective, the observations with subsequent changes in satellite orbital altitude during the GOCE LOA period are more sensitive to the gravity field signals. Pail [24]

theoretically demonstrated the benefits of increasing observation volume and reducing orbital altitude for enhancing precision in gravity field modeling. However, there is a limited research that quantitatively analyzes the contributions of SGG data at different orbital altitudes when constructing combined static gravity field models based on real GOCE measurements, especially during the four-orbit reduction operations in the LOA stage.

Therefore, using the reprocessed GOCE Level-1B SGG data from GOCE HPF,[2] we constructed the SGG normal equation up to 300 d/o through a direct approach. By further incorporating GRACE satellite data and applying regularization constraints, we derived the Tongji-GMMG2021S combined static gravity field model up to 300 d/o. Subsequently, an analysis was conducted on the contributions of SGG data at different orbital altitudes to the Tongji-GMMG2021S model.

The rest of this article is organized as follows. Section II briefly presents the theory behind utilizing SGG data for gravity field estimation and its joint inversion with GRACE satellite data. In Section III, the strategy for solving the Tongji-GMMG2021S model is introduced and evaluated using the latest combined GOCE/GRACE models and GNSS/Leveling data. The contribution of SGG data at different orbital altitudes to the Tongji-GMMG2021S solution is examined in Section IV. Section V concludes this article.

II. THEORETICAL METHODS FOR THE SATELLITE GRAVITY FIELD ESTIMATION

The gravitational potential $V(\theta, \lambda, r)$ of any point in the Earth's outer space can be mathematically expressed as follows within the framework of the spherical coordinate system [25]:

$$V(\theta, \lambda, r) = \frac{GM_\oplus}{r} \left[1 + \sum_{l=2}^{N} \left(\frac{a}{r}\right)^l \sum_{m=0}^{l} \left(\bar{C}_{l,m} \cos m\lambda \right.\right.$$
$$\left.\left. + \bar{S}_{l,m} \sin m\lambda \right) \bar{P}_{l,m}\left(\cos\theta\right) \right] \qquad (1)$$

where G denotes the universal gravitational constant; $M_\oplus$ represents the mass of the Earth; a is the semimajor axis of the reference ellipsoid; (θ, λ, r) denote the geocentric colatitude, geocentric longitude, and geocentric radius of the given point, respectively; $\bar{P}_{l,m}(\cos\theta)$ is the fully normalized associated Legendre function for the degree l and order m; $(\bar{C}_{l,m}, \bar{S}_{l,m})$ are the fully normalized spherical harmonic coefficients; and N indicates the maximum degree for computing the gravitational potential.

A. Normal Equation for the SGG Observations

The direct approach, as one of its advantages, establishes the observation equation for SGG within the gradiometer reference frame (GRF) system at each epoch, enabling the estimation of gravity field parameters based on gravity gradient observations at the normal equation level [7], [22]. The normal equation is constructed by incorporating a bandpass filter, effectively

---

[2][Online]. Available: https://goce-ds.eo.esa.int/oads/access/collection.

accounting for color noise in the observation series. Therefore, this study employs this approach to solve static gravity field models based on SGG data. In the Earth fixed reference frame, the gravitational potential gradients can be derived by taking the second-order derivatives of (1). However, the GOCE SGG data are expressed in the GRF, and the *Vxy* and *Vyz* components show lower accuracy [6], [26]. Any conversion between different reference frames may result in an amplification of observation errors in the target reference frame. Therefore, the SGG observation equation is established in the GRF as follows [7], [13], [18], [19]:

$$l_{\text{SGG}} = A_{\text{SGG}} \, \delta u + e_{\text{SGG}} \qquad (2)$$

where A_{SGG} represents the design matrix for the gravity field parameters; $\delta u = (\delta \bar{C}_{l,m}, \delta \bar{S}_{l,m})$ are the corrections to a priori spherical harmonic coefficients; l_{SGG} denotes the residual SGG vector for applicable components (i.e., *Vxx*, *Vyy*, *Vzz*, and *Vxz*) obtained by subtracting their reference values computed from the priori spherical harmonic coefficients; and e_{SGG} is the error vector. Since the SGG data are dominated by the correlated noise at frequencies below 0.005 Hz [7], (2) is subjected to a filtering operation as follows:

$$F\{l_{\text{SGG}}\} = F\{A_{\text{SGG}}\} \delta u + F\{e_{\text{SGG}}\} \qquad (3)$$

where $F\{\}$ represents the filtering operation. Using the least-squares adjustment, the SGG normal equation can be derived as follows:

$$N_{\text{SGG}} \delta u = w_{\text{SGG}} \qquad (4)$$

where $N_{\text{SGG}} = F\{A_{\text{SGG}}\}^T \, PF\{A_{\text{SGG}}\}$ is the SGG normal matrix; $w_{\text{SGG}} = F\{A_{\text{SGG}}\}^T \, PF\{l_{\text{SGG}}\}$ is the right-hand vector; and P represents the weight matrix for the filtered SGG observations, which is an identity matrix due to the application of the filter.

B. GOCE/GRACE Combined Normal Equations and Regularization

A GOCE sun-synchronous orbit with an inclination of 96.7° results in a polar gap of 6.7°, which is the primary reason for the severe ill-conditioned characteristics of the normal equation derived from GOCE observations [27], [28]. Therefore, the integration of SGG and GRACE data is necessary for solving the static gravity field model due to the highly accurate long-wavelength signals provided by GRACE observations. In this study, the Tongji-Grace02s normal equation of GRACE observations constructed using a modified short-arc approach is directly used. More details can be found in Chen et al. [29]. Furthermore, we also introduce the Kaula regularization matrix [30], [31] to enhance the stability of coefficients at high degrees and orders. The expression for combining the SGG and GRACE data, as well as the Kaula regularization matrix, is as follows:

$$\frac{\sigma_0^2}{\sigma_{\text{SGG}}^2} N_{\text{SGG}} + \frac{\sigma_0^2}{\sigma_{\text{GRACE}}^2} N_{\text{GRACE}} + \alpha K$$
$$= \frac{\sigma_0^2}{\sigma_{\text{SGG}}^2} w_{\text{SGG}} + \frac{\sigma_0^2}{\sigma_{\text{GRACE}}^2} w_{\text{GRACE}} \qquad (5)$$

where the unit weight factor is represented by σ_0, while the variances for the SGG and GRACE normal equations $\sigma_*^2 (* = \text{SGG, GRACE})$ are determined using the variance component estimation (VCE) method; N_* denotes the normal matrices; w_* are the right-side vector of the normal equations; the Kaula regularization matrix is denoted as K; and the corresponding regularization parameter α is determined by using the generalized cross-validation (GCV) approach [28].

III. DEVELOPMENT OF THE TONGJI-GMMG2021S SOLUTION

A. Data Processing

Before deriving static gravity field models, the GOCE Level 1B SGG observations should undergo a series of data processing steps, including

1) correcting the temporal gravity field variations;
2) detecting and screening outliers in the dataset; and
3) applying decorrelation filtering techniques.

The data processing workflow for the Tongji-GMMG2021S model is illustrated in Fig. 1.

Additional clarification is needed for Fig. 1.

1) The input data includes gravity gradients in the GRF system (EGG_GGT_1i), gradiometer inertial attitude quaternions (EGG_IAQ_1i) used for transforming SGG from GRF to Inertial Reference Frame, and Reduced-Dynamic orbits (SST_PRD_2) used for geo-locating the SGG measurements.
2) We subtract both the tidal and nontidal temporal variations in the gravity gradients using background force models.
3) The outliers in SGG data can be classified into two distinct types, namely block and discrete outliers. To identify block outliers, a time window of one day is used. On the other hand, the detection of discrete outliers is performed by using a moving window of 90 min, which approximately corresponds to one orbit cycle revolution. It should be noted that when there is a significant number of consecutive outliers or missing epochs, the continuous interpolation of data may have an impact on the subsequent determination of gravity field models. Therefore, in this study, interpolation is only performed for missing epochs or continuous outliers lasting less than 40 s; for intervals or outliers exceeding 40 s, the dataset is divided into multiple segments.
4) The segmented SGG data undergo an 8th-order infinite impulse response bandpass filter within the frequency range of 0.005–0.125 Hz, excluding the warming-up data length of 5400 for each segment during the inversion process used for gravity field models.
5) The components of *Vxx*, *Vyy*, *Vzz*, and *Vxz* are incorporated with equal weighting assigned for each segment.
6) The integration of the GRACE observations enhances the accuracy of the spherical harmonic coefficients at lower degrees.

To address the ill-posed nature of the satellite gravity field inversion at higher degrees, taking into account the validation result from published models (i.e., GO_CONS_GCF_2_DIR_R6,
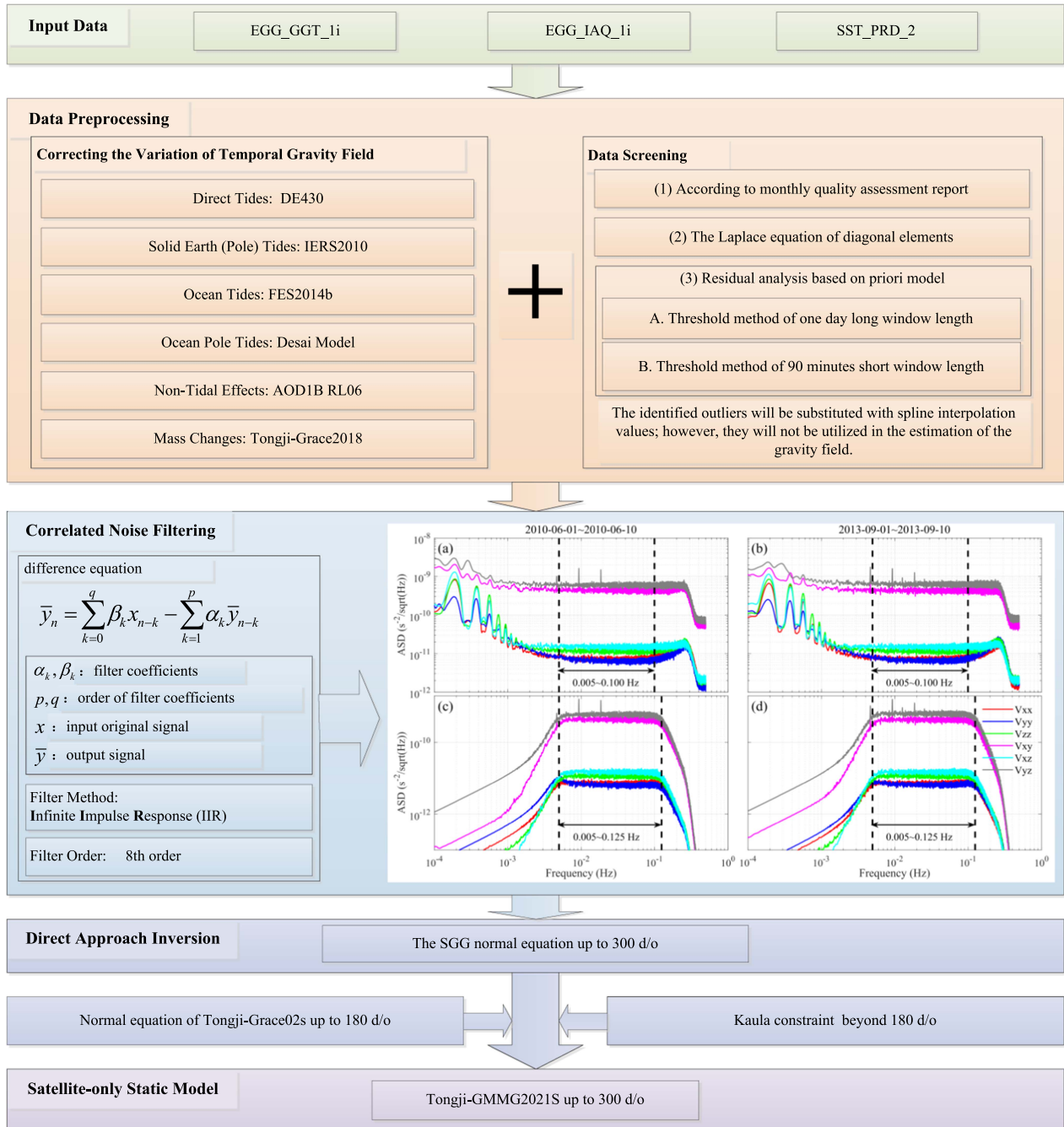
Fig. 1.   Data processing workflow for Tongji-GMMG2021S solution.

and GO_CONS_GCF_2_TIM_R6), we apply the Kaula regularization to the coefficients beyond 180 d/o [9]. As a consequence, the Tongji-GMMG2021S satellite-only static gravity field model has been developed and published on the ICGEM website.[3]

B. Comparison of Tongji-GMMG2021S

The GO_CONS_GCF_2_DIR_R6, GOCO06s, and WHU-SWPU-GOGR2022S models have been selected for comparison with the Tongji-GMMG2021S model in terms of GDV relative

to XGM2019. These models all utilize reprocessed GOCE SGG data from ESA GOCE HPF and GRACE data but employ different processing strategies, are illustrated in Fig. 2.

The following deductions can be drawn from Fig. 2: 1) For lower degrees, noticeable discrepancies are observed among different models, primarily due to unmodeled time-variable signals and varying reference epochs employed in the models [29]; however, above 180 d/o, all four models demonstrate good agreement with each other. 2) At a half-wavelength of 100 km (approximately 200 d/o), the GDV relative to XGM2019 is less than 1 cm across all four models. The error characteristics of each
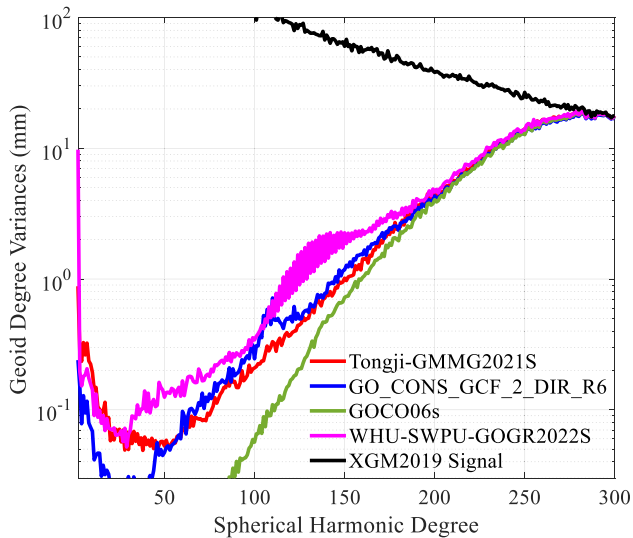
Fig. 2.   GDV of Tongji-GMMG2021S and other GOCE/GRACE combined models w.r.t. XGM2019.

model are further compared in the spatial domain using $1° \times 1°$ gravity anomaly grids (excluding the polar gaps) with respect to the XGM2019 model truncated to 300 d/o, as illustrated in Fig. 3.

The four models exhibit consistent error characteristics not only in the spectral domain but also in the spatial domain, with standard deviations of 7.39, 6.82, 7.36, and 7.43 mGals for the Tongji-GMMG2021S, GO_CONS_GCF_2_DIR_R6, GOCO06s, and WHU-SWPU-GOGR2022S models, respectively. Errors on land generally exhibit larger than those over the ocean. Notably significant discrepancies are mainly observed along coastlines and complex terrain areas such as the Tibetan Plateau. These disparities primarily arise from variations in data sources between the GOCE/GRACE combined models and the XGM2019 solution [32]. The incorporation of the ground gravity dataset from the US National Geospatial-Intelligence Agency into the XGM2019 model [32] provides additional information that cannot be obtained solely from the GOCE SGG and GRACE satellite observations.

C. Validation of Tongji-GMMG2021S

Independent validation of the aforementioned gravity field models is conducted by employing the Global Navigation Satellite System (GNSS) and Leveling data. To perform this validation, the geoid heights derived from the four models are subtracted from the diverse GNSS/Leveling datasets from the National Geodetic Survey[4] across regions of the United States (8006 points), Canada (212 points), and Mexico (536 points), as illustrated in Fig. 4. The standard deviations of the differences in Fig. 4(a)–(c) correspond to different truncated degrees for each model, aligning with the evaluation method used by the ICGEM service agency. The discrepancies between the geoid

heights calculated from gravity field models truncated to different degrees and GNSS/leveling data are subsequently utilized for calculating the standard deviations.

Fig. 4(a)–(c) illustrates the discrepancies between the GNSS/Leveling data and the GOCE/GRACE combined models truncated to different degrees, encompassing errors originating from both GNSS data and unmodeled short-wavelength gravity field signals. As shown in Fig. 4(a)–(c), gradually increasing the degree to be truncated leads to a decrease in their standard deviations. This can be attributed to the inclusion of gravity field signals with higher degrees, as the GNSS/leveling data contain full-frequency gravity field information. In other words, short-wavelength signals of gravity field models should not be disregarded during independent validation [33].

To account for the short-wavelength gravity field signals, the coefficients beyond the truncated degrees are extended up to 2160 d/o by using the XGM2019e model [32]. As illustrated in Fig. 4(d)–(f), the accuracy levels are generally consistent before degree 200. However, beyond degree 200, the standard deviations gradually increase due to variations in the sensitivity of SGG data to high-degree gravity field signals. Despite differences in solution strategies, all models demonstrate similar noise characteristics. The disparities in standard deviations between Tongji-GMMG2021S and other combined GOCE/GRACE models are all less than 1 cm. Overall, the validation results of the Tongji-GMMG2021S model provide sufficient evidence to support the analysis of how a reduced GOCE orbital altitude impacts gravity field estimation based on SGG data.

IV. ANALYSIS OF THE CONTRIBUTION OF THE REDUCED ORBITAL ALTITUDE OBSERVATIONS

In this study, the daily average value of the GOCE orbital altitude is computed based on the reduced-dynamic orbits (SST_PRD_2) published by the GOCE HPF.[5] As shown in Fig. 5, the orbital altitude primarily underwent two distinct phases throughout the GOCE scientific mission. The first phase denoted as the HOA period, was characterized by a mean altitude of 259.5 km. Subsequently, to enhance scientific output and optimize the quality of observations, ESA implemented a series of orbital adjustments during the LOA period. Specifically, these adjustments involved a progressive decrease in orbital altitudes by 8.5, 6.5, and 5.5 km, respectively, followed by a subsequent reduction of 10 km resulting in a mean altitude of 229.0 km.

During the LOA period, we conduct a comprehensive analysis of SGG data to assess its contribution to static gravity field solutions. This analysis takes into account factors such as the frequency-error characteristics of the observations, contributions of the SGG data at the normal matrix level, comparisons with GDV, discrepancies in spectral errors, and spatial gravity anomalies of the derived gravity field models relative to the reference model.

---

[4][Online]. Available: https://geodesy.noaa.gov/.

[5][Online]. Available: https://goce-ds.eo.esa.int/oads/access/collection.
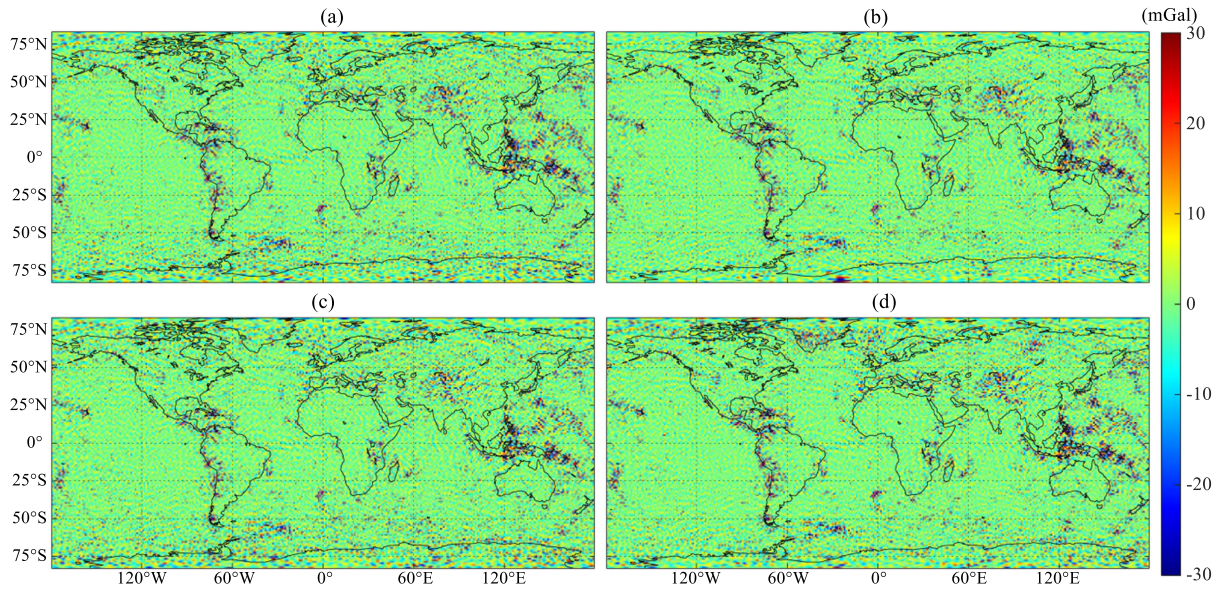
Fig. 3. Comparison of spatial errors in terms of gravity anomalies between different GOCE/GRACE combined models and the XGM2019 model. (a) Tongji-GMMG2021S. (b) GO_CONS_GCF_2_DIR_R6. (c) GOCO06s. (d) WHU-SWPU-GOGR2022S.
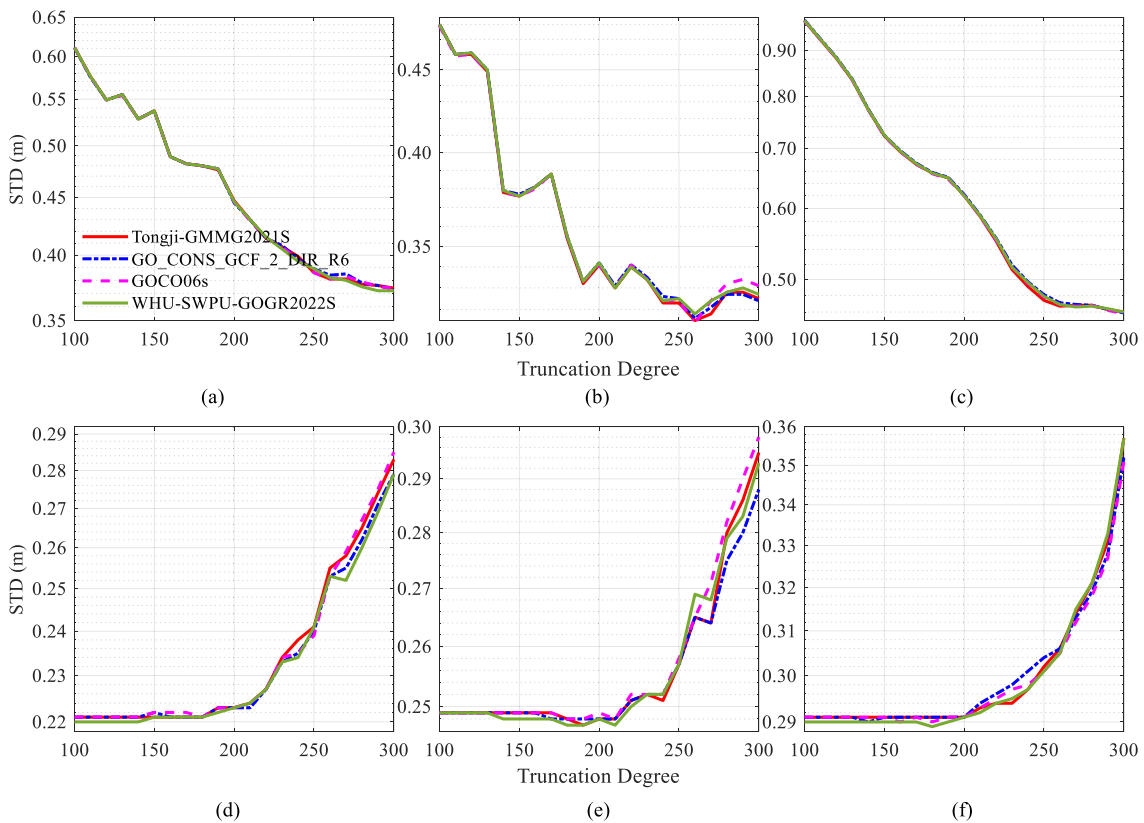

Fig. 4. Statistical differences between the GNSS/Leveling data and the GOCE/GRACE combined models. (a) USA. (b) Canada. (c) Mexico. (d) USA. (e) Canada. (f) Mexico.

A. Frequency Characteristics of the SGG Observations

The daily variations (excluding data anomalies) in the four components (Vxx, Vyy, Vzz, and Vxz) since July 2012 are depicted in Fig. 6(a)–(d). The signal strength (absolute value) of the Vxx and Vzz components shows a gradual increase, as

shown in Fig. 6(a) and (c). These findings indicate that variations in orbital altitudes result in changes in the sensitivity of SGG data towards gravity field signals. Theoretically, it is expected that the trace of the gradient tensor would be zero; however, empirical evidence contradicts this assumption [6], [26]. This inconsistency may potentially explain the observed ascending
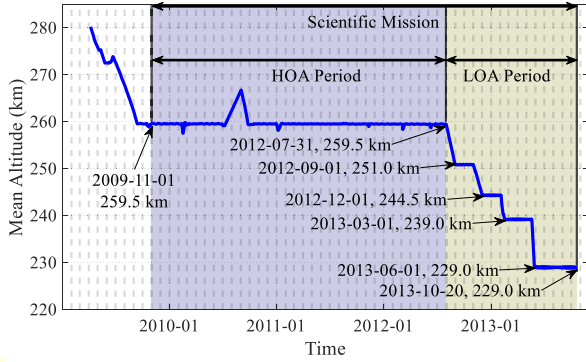
Fig. 5. GOCE scientific mission orbital altitude overview.

pattern in the *Vyy* component. Therefore, additional research is necessary to determine its exact underlying cause in the near future. As for the *Vxz* component, the signal slightly increases as orbital altitude decreases.

Fig. 6(e)–(h) shows the amplitude spectral densities (ASDs) of the residuals obtained by subtracting the Tongji-GMMG2021S-based gradients from the observations with the components *Vxx*, *Vyy*, *Vzz*, and *Vxz*, which are typically considered as noise. The noise frequency characteristics remain unchanged as the orbital altitude decreases, while the signals become stronger, as depicted in Fig. 6. In other words, the reduction in the orbital altitudes results in an improved signal-to-noise ratio. Within the effective observation frequency range 0.005–0.1 Hz, both *Vxx* and *Vyy* components demonstrate noise levels of approximately 10 mE (1 mE $= 10^{-3}$ E $= 10^{-12}$ s^{-2}). In contrast, the noise levels for *Vzz* and *Vxz* components are approximately 20 mE.

B. Contribution Factors of the Observations and Regularization Matrix

Due to the decrease in the GOCE orbital altitude, it is expected that the nature of the corresponding normal matrix is expected to vary during distinct phases. As depicted in Fig. 7, the contributions of SGG data to the normal matrix of Tongji-GMMG2021S are computed based on (6) during both the HOA and LOA stages:

$$\boldsymbol{R}_i = \boldsymbol{N}^{-1} \left(\frac{\sigma_0^2}{\sigma_i^2} \right) \boldsymbol{N}_i; \; r_{i(k)} = [\boldsymbol{R}_i]_{kk} \tag{6}$$

where $\boldsymbol{N}$ represents the combined normal matrix; $\boldsymbol{N}_i$ represents the ith normal matrix, such as the SGG data, GRACE data, and Kaula regularization matrix; $\boldsymbol{R}_i$ denotes the ith contribution matrix; and the term $r_{i(k)}$ corresponding to the kth diagonal element in the contribution matrix is treated as the contribution factor for each degree and order [10], [20].

According to the (6), it is evident that the variance σ_i^2 of the ith matrix has a significant influence on the contribution matrix, while the unit weight factor has no impact on it. However, this study primarily focuses on investigating the contributions of different data factors to Tongji-GMMG2021S. In principle, to reasonably account for the difference in accuracy between GRACE data and GOCE SGG data, the corresponding weighting factors for GRACE satellite data and GOCE SGG data

should be estimated using the VCE method, while the regularization parameter is determined through the GCV method. Consequently, all variance factors for the data are uniquely determined, ensuring the validity of the analysis results in this study.

As shown in Fig. 7, the GRACE contribution primarily focuses on geopotential coefficients below 95 d/o, particularly below 36 d/o. These results indicate that the combined solution is mainly influenced by the GRACE data at low degrees. Furthermore, the Kaula regularization matrix plays a significant role in enhancing the stability of the normal matrix beyond 260 d/o. The contribution of SGG data to the Tongji-GMMG2021S model ranges from 95 to 260 degrees, with a substantial contribution ratio exceeding 50%. These findings also align well with previous studies conducted by Kvas et al. [10] and Pail et al. [16]. However, it is important to note that the contributions of SGG observations to Tongji-GMMG2021S vary across different orbital altitudes and periods. Despite the longer duration of the HOA period compared to the LOA period, the latter demonstrates a significantly greater contribution beyond 112 d/o than the former. However, both periods demonstrate comparable contributions below 112 d/o, indicating that lower orbital altitudes are more sensitive to the signals at higher degrees and orders.

To comprehensively quantify the contributions of various factors, Fig. 8 illustrates the relative contribution ratios of each factor to Tongji-GMMG2021S at different degrees. Notably, both Figs. 7 and 8 demonstrate that beyond degree 112, the 15-month observations during the LOA phase contribute more significantly to the combined normal matrix than the 30-month data in the HOA stage, with a mean orbital altitude of 259.5 km. These findings highlight that as the orbital altitude decreases, the sensitivity towards the medium and high degrees of gravity field signals increases.

C. Contribution Analysis at the Normal Matrix Level

Considering the significant impact of the decreased orbital altitudes between August 2012 and October 2013 on the normal matrix of Tongji-GMMG2021S, the contribution ratio of the SGG data at the normal matrix level for each month from July 2012 to October 2013 is further examined. Following (6), the subsequent average contribution ratio per degree for each month is illustrated in Fig. 9. In general, the contribution of SGG data to gravity field modeling gradually increases as the orbital altitude decreases, primarily within the range of 112–260 degrees. Notably, during the final 5 months of observations, the total contribution for each degree between 150 and 260 exceeded 25%, with the highest contribution reaching 38% at degree 221. Throughout the period from March to October 2013, a consistent total contribution exceeding 31% was observed for each degree within the range of 150–260. However, data availability in 2013 was limited due to orbital adjustment events and data quality issues, particularly in February and May 2013. As a result, the contribution from observations collected at similar orbital altitudes during these months is relatively smaller. This case depends upon satellite calibration operations, special events,
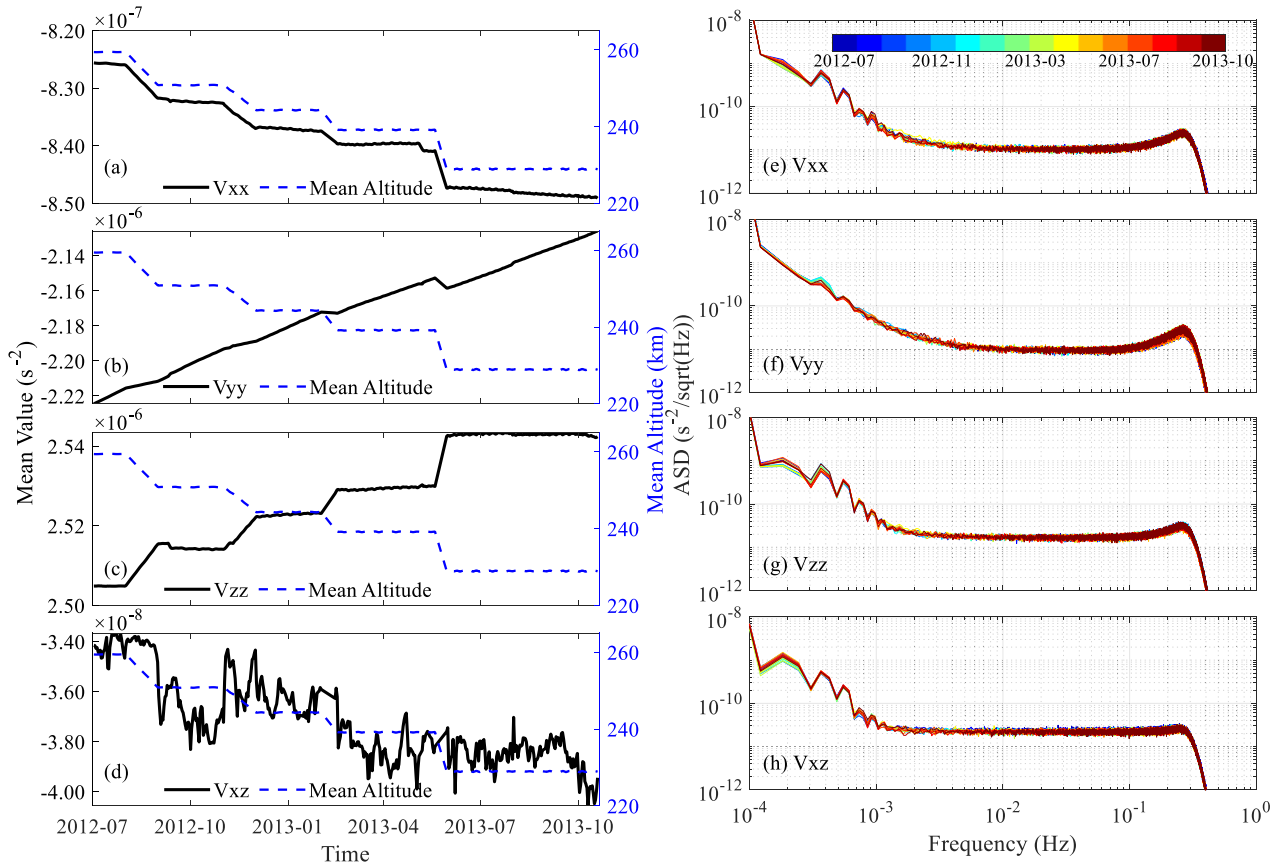
Fig. 6. Daily mean values of the four components in the GRF system (left column) and ASDs of the residuals for the SGG four components (right column).
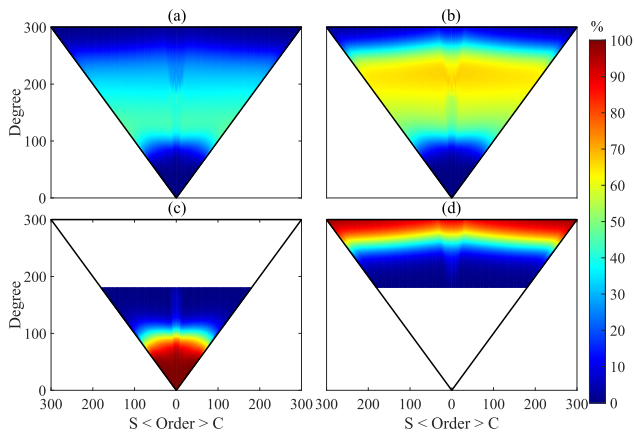

Fig. 7. Contributions of various factors to the normal matrix of Tongji-GMMG2021S. (a) HOA Period SGG. (b) LOA Period SGG. (c) GRACE. (d) Kaula.

Fig. 8. Average contribution ratios of the various factors to the Tongji-GMMG2021S model.

and data anomalies. For more detailed information, please refer online.[6]

D. Contribution Assessment in the Spectral Domain

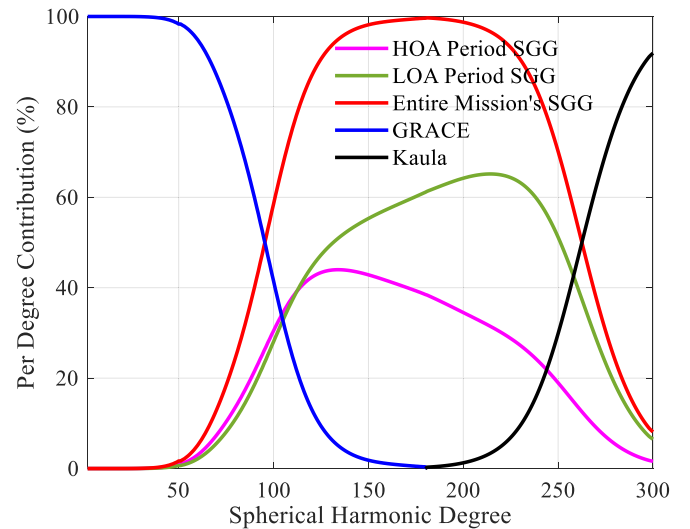To conduct a spectral analysis of the gravity field models derived from the SGG data at the HOA and LOA periods, we obtain two corresponding gravity field solutions. During this process, we also apply the Kaula regularization, incorporate the normal equation of Tongji-Grace02s, and ensure consistency with the weighting factor of the Tongji-GMMG2021S model.

Subsequently, we compute the GDV with respect to XGM2019 using the GOCE/GRACE combined model and the
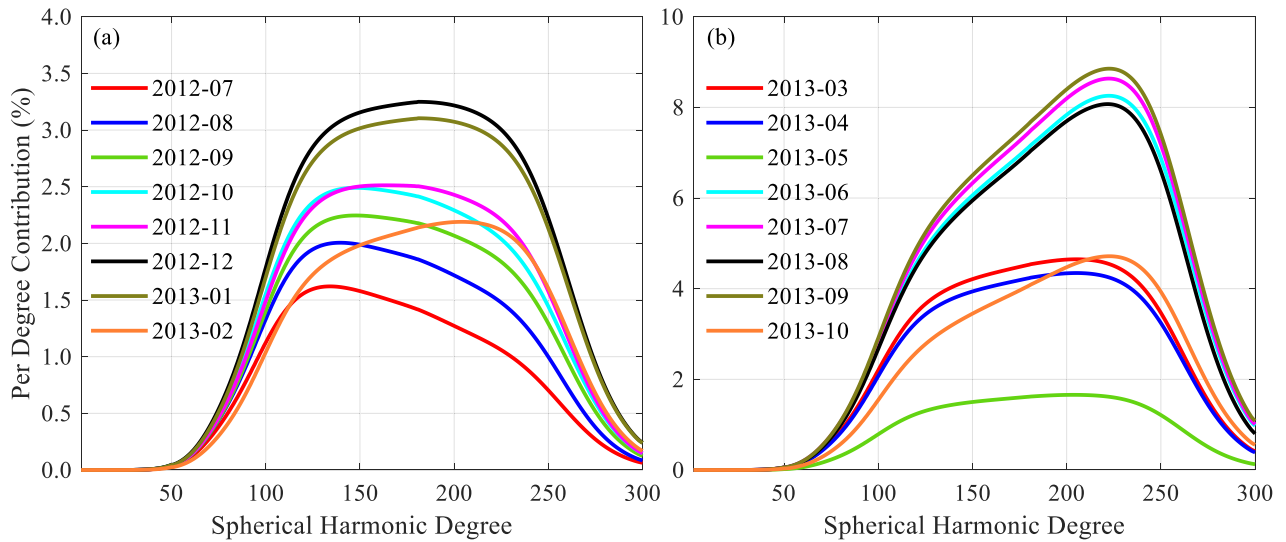
Fig. 9. Monthly average SGG contribution per degree from July 2012 to October 2013.
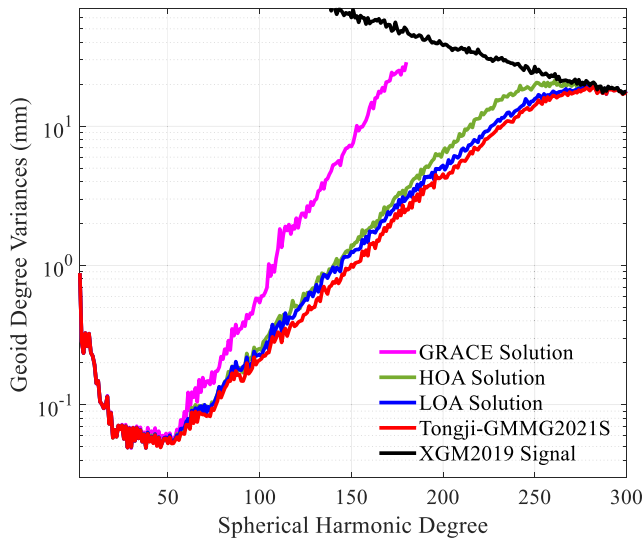

Fig. 10. GDV values of various models w.r.t. XGM2019.

TABLE I
CUMULATIVE GDV VALUES OF VARIOUS MODELS W.R.T. XGM2019 (IN UNIT OF MM)

Truncation (d/o)	GRACE Solution	HOA Solution	LOA Solution	Tongji-GMMG2021S
100	2.31	1.61	1.59	1.53
140	16.56	4.13	3.89	3.26
180	104.58	14.40	12.73	10.57
200	--	27.15	22.67	19.24
220	--	48.68	37.52	31.99
260	--	120.54	93.50	83.71
300	--	171.28	148.17	139.77

GRACE-only model (Tongji-Grace02s), as shown in Fig. 10. Compared with the GRACE-only model, the integration of GRACE and SGG data significantly reduces the GDV beyond 72 d/o. The cumulative GDV values up to various degrees are further given in Table I, demonstrating that the combined model yields a significantly smaller cumulative GDV compared to the GRACE-only solution. Despite utilizing a larger amount of SGG data during the HOA period than during the LOA period, the decreased orbital altitudes in the latter stage significantly reduce the GDV values. These further emphasize the importance of SGG observations at lower orbital altitudes for accurately estimating the gravity field, particularly beyond 180 d/o.

E. Significance Analysis in the Spatial Domain

We further conduct a spatial domain analysis of the solution obtained during the two distinct mission stages, i.e., HOA and LOA. The geoid height error grids, with a spatial resolution of 1° × 1° (excluding polar gaps) for both HOA and LOA solutions relative to the Tongji-GMMG2021S model up to 300 d/o are shown in Fig. 11. As shown in Fig. 11, the LOA solution demonstrates an error reduction compared to the HOA solution. The standard deviation of the grids during the LOA stage is approximately 7.24 cm. In contrast, the spatial pattern of the HOA model is significantly contaminated by errors, resulting in a standard deviation of 14.82 cm. Despite the limited availability of data in the LOA stage compared to the HOA stage, there is a reduction of 51.15% in the standard deviation of the geoid height errors during the LOA stage. Therefore, the observations during the LOA stage contribute more substantially to Tongji-GMMG2021S than those in the HOA stage.

V. CONCLUSION

The GOCE mission has played an important role in the development of high-resolution and high-precision static Earth gravity field models. Following the successful completion of the nominal objectives of the GOCE satellite, its orbital altitude decreased from 259.5 to 229.0 km during the final 15 months, which improved the sensitivity of SGG data to gravity field signals. Conducting quantitative analysis on the contribution of the SGG data at different orbital altitudes to gravity field modeling is important for refining high-precision static gravity
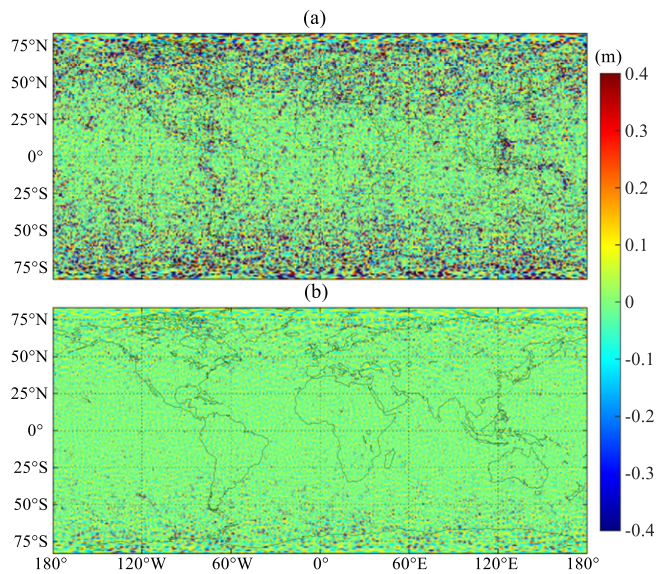
Fig. 11. Geoid height errors of the (a) HOA and (b) LOA solutions w.r.t Tongji-GMMG2021S. (a) SGG HOA Period. (b) SGG LOA Period.

field solutions and designing next-generation SGG-type gravity satellite missions. Therefore, utilizing the reprocessed Level-1B SGG data from ESA GOCE HPF and GRACE satellite data, we successfully constructed the Tongji-GMMG2021S gravity field model up to 300 d/o. Subsequently, we conducted an extensive investigation into the variations in signal and noise characteristics within the SGG data, as well as their respective contributions to the Tongji-GMMG2021S model from multiple perspectives encompassing the normal matrix, spectral domain, and spatial domain. The following conclusions can be drawn from our analysis.

1) The accuracy of the Tongji-GMMG2021S solution was comparable to that of the latest combined GOCE/GRACE models.
2) With decreasing orbital altitude, an overall signal enhancement in the SGG data was observed, while the noise remained at a constant level, resulting in an improved signal-to-noise ratio.
3) Based on the contribution analysis at the normal matrix level, a decrease in orbital altitude corresponds to an increase in the accuracy of derived gravity field models, particularly at medium and high degrees. Notably, during the last 5 months of the SGG observations at a mean orbital altitude of 229.0 km, the contribution exceeded 25% between degrees 150 and 260. Moreover, from March 2013 to October 2013, the contribution exceeded 31% within the degree range of 150–260.
4) In the spectral domain, the joint solution derived from both SGG data and GRACE data exhibited a smaller GDV beyond degree 72 compared to the GRACE-only solution. In addition, during the LOA period, the solution derived from SGG data exhibited a greater advantage over that obtained during the HOA period beyond 180 d/o.
5) In the spatial domain, despite having fewer available data in the LOA period, the corresponding solution exhibited a

standard deviation of 7.24 cm with respect to the Tongji-GMMG2021S solution, which significantly reduced geoid height errors by 51.15% compared to those derived from the HOA period (with a standard deviation of 14.82 cm).

REFERENCES

[1] J. Kusche, V. Klemann, and N. Sneeuw, "Mass distribution and mass transport in the earth system: Recent scientific progress due to interdisciplinary research," *Surv. Geophys.*, vol. 35, no. 6, pp. 1243–1249, 2014.
[2] R. Pail et al., "Science and user needs for observing global mass transport to understand global change and to benefit society," *Surv. Geophys.*, vol. 36, no. 6, pp. 743–772, 2015.
[3] J. Chen et al., "Applications and challenges of GRACE and GRACE follow-on satellite gravimetry," *Surv. Geophys.*, vol. 43, no. 1, pp. 305–345, 2022.
[4] B. Elsaka, A. Alothman, and W. Godah, "On the contribution of GOCE satellite-based GGMs to improve GNSS/leveling geoid heights determination in Saudi Arabia," *IEEE J. Sel. Topics Appl. Earth Observ. Remote Sens.*, vol. 9, no. 12, pp. 5842–5850, Dec. 2016.
[5] C. Xiao et al., "Monitoring the catastrophic flood with GRACE-FO and near-real-time precipitation data in northern Henan province of China in July 2021," *IEEE J. Sel. Topics Appl. Earth Observ. Remote Sens.*, vol. 16, pp. 89–101, 2023.
[6] R. Floberghagen et al., "Erratum to: Mission design, operation and exploitation of the gravity field and steady-state ocean circulation explorer (GOCE) mission," *J. Geodesy*, vol. 86, no. 3, pp. 241–241, 2012.
[7] R. Pail et al., "First GOCE gravity field models derived by three different approaches," *J. Geodesy*, vol. 85, no. 11, pp. 819–843, 2011.
[8] C. Siemes, M. Rexer, A. Schlicht, and R. Haagmans, "GOCE gradiometer data calibration," *J. Geodesy*, vol. 93, no. 9, pp. 1603–1630, 2019.
[9] C. Förste et al., "ESA's release 6 GOCE gravity field model by means of the direct approach based on improved filtering of the reprocessed gradients of the entire mission (GO_CONS_GCF_2_DIR_R6)," *GFZ Data Serv.*, 2019, doi: 10.5880/ICGEM.2019.004.
[10] A. Kvas et al., "GOCO06s – a satellite-only global gravity field model," *Earth Syst. Sci. Data*, vol. 13, no. 1, pp. 99–118, 2021.
[11] J. Chen et al., "Static gravity field recovery and accuracy analysis based on reprocessed GOCE level 1b gravity gradient observations," in *Proc. EGU Gen. Assem.*, May 2022, Paper EGU22-6771.
[12] Y. Zhao et al., "Determination of static gravity field model by using satellite data of GOCE and GRACE," *Chin. J. Geophys.*, vol. 66, no. 6, pp. 2322–2336, 2023.
[13] J. M. Brockmann, T. Schubert, and W.-D. Schuh, "An improved model of the Earth's static gravity field solely derived from reprocessed GOCE data," *Surv. Geophys.*, vol. 42, no. 2, pp. 277–316, 2021.
[14] X. Xu et al., "A GOCE only gravity model GOSG02S based on the SGG and SST observations," *GFZ Data Serv.*, 2023, doi: 10.5880/icgem.2023.002.
[15] P. Zingerle et al., "The polar extended gravity field model TIM_R6e," *GFZ Data Serv.*, 2019, doi: 10.5880/ICGEM.2019.005.
[16] R. Pail et al., "Combined satellite gravity field model GOCO01S derived from GOCE and GRACE," *Geophysical Res. Lett.*, vol. 37, no. 20, 2010, Art. no. L20314.
[17] H. H. Farahani et al., "The static gravity field model DGM-1S from GRACE and GOCE data: Computation, validation and an analysis of GOCE mission's added value," *J. Geodesy*, vol. 87, no. 9, pp. 843–867, 2013.

[18] W. Yi, "The Earth's gravity field from GOCE. Germany," Technische Universität Mänchen, Munich, Germany, 2011.

[19] H. Wu, "Gravity field recovery from GOCE observations," Fachrichtung Geodäsie und Geoinformatik der Leibniz Universität Hannover, Hanover, Germany, 2016.

[20] W. Yi, R. Rummel, and T. Gruber, "Gravity field contribution analysis of GOCE gravitational gradient components," *Studia Geophysica et Geodaetica*, vol. 57, no. 2, pp. 174–202, 2013.

[21] S. L. Bruinsma et al., "Comparison of satellite-only gravity field models constructed with all and parts of the GOCE gravity gradient dataset," *Mar. Geodesy*, vol. 39, no. 3-4, pp. 238–255, 2016.

[22] S. L. Bruinsma et al., "ESA's satellite-only gravity field model via the direct approach based on all GOCE data," *Geophysical Res. Lett.*, vol. 41, no. 21, pp. 7508–7514, 2014.

[23] GOCE Flight Control Team, "GOCE end-of-mission operations report," European Space Agency, Tech. Rep. GO-RPESC-FS-6268, 2014. [Online]. Available: https://earth.esa.int/documents/10174/85857/2014-GOCE-Flight-Control-Team.pdf

[24] R. Pail, "It's all about statistics: Global gravity field modeling from GOCE and complementary data," in *Handbook of Geomathematics*, W. Freeden, M. Z. Nashed, and T. Sonar, Eds., Berlin, Germany: Springer, 2015, pp. 2345–2372.

[25] W. A. Heiskanen and H. Moritz, *Physical Geodesy*. San Francisco, CA, USA: Freeman, 1967.

[26] R. Rummel, W. Yi, and C. Stummer, "GOCE gravitational gradiometry," *J. Geodesy*, vol. 85, no. 11, pp. 777–790, 2011.

[27] S. Rudolph, J. Kusche, and K. H. Ilk, "Investigations on the polar gap problem in ESA's gravity field and steady-state ocean circulation explorer mission (GOCE)," *J. Geodynamics*, vol. 33, no. 1, pp. 65–74, 2002.

[28] J. Kusche and R. Klees, "Regularization of gravity field estimation from satellite gravity gradients," *J. Geodesy*, vol. 76, no. 6, pp. 359–368, 2002.

[29] Q. Chen et al., "Tongji-Grace02s and Tongji-Grace02k: High-precision static GRACE-only global earth's gravity field models derived by refined data processing strategies," *J. Geophysical Res., Solid Earth*, vol. 123, no. 7, pp. 6111–6137, 2018.

[30] W. M. Kaula, *Theory of Satellite Geodesy*. New York, NY, USA: Dover, 1966.

[31] P. Ditmar, J. Kusche, and R. Klees, "Computation of spherical harmonic coefficients from gravity gradiometry data to be acquired by the GOCE satellite: Regularization issues," *J. Geodesy*, vol. 77, no. 7, pp. 465–477, 2003.

[32] P. Zingerle, R. Pail, T. Gruber, and X. Oikonomidou, "The combined global gravity field model XGM2019e," *J. Geodesy*, vol. 94, no. 7, 2020, Art. no. 66.

[33] T. Gruber and M. Willberg, "Signal and error assessment of GOCE-based high resolution gravity field models," *J. Geodetic Sci.*, vol. 9, no. 1, pp. 71–86, 2019.

Qiujie Chen received the B.S. degree in surveying and mapping engineering from the Guangdong University of Technology, Guangzhou, Guangdong, China, in 2011, and the Ph.D. degree in geodesy from Tongji University, Shanghai, China, in 2016.

He is currently a Professor with the College of Surveying and Geo-Informatics, Tongji University. His research interests include short-arc approach for satellite-based gravity field determination, frequency-dependent noise modeling, non-gravitational acceleration calibration, regularization methodologies, mascon modeling, and simulations for next-generation gravity satellites.

Yunzhong Shen received the Ph.D. degree in geophysical geodesy from the Institute of Geodesy and Geophysics, Chinese Academy of Sciences, Beijing, China, in 2000.

He is currently a Professor with the College of Surveying and Geo-informatics, Tongji University, Shanghai, China. His research interests include geodetic data processing on satellite gravimetry and satellite positioning. His main research interests include the regularized solution to the ill-conditioned inverse problem of recovering a gravitational potential model from satellite-to-satellite tracking data, as well as variance component and parameter estimation theory.

Dr. Shen is an Editor of *Journal of Geodesy* and *Acta Geodetica et Cartographica Sinica*.

Jianhua Chen received the Master's degree in surveying and mapping engineering from the Guangdong University of Technology, Guangzhou, China, in 2022. He is currently working toward the Ph.D. degree in geodesy with the College of Surveying and Geo-informatics, Tongji University, Shanghai, China.

His research interests include satellite-based gravity field determination, simulation of next-generation gravity missions, and the application of gravity field model.

Xingfu Zhang received the B.S. degree in surveying and mapping engineering from the Jilin University, Changchun, China, in 2001, and the Ph.D. degree in geodesy from Tongji University, Shanghai, China, in 2007.

He is currently a Professor with the Department of Civil and Transportation Engineering, Guangdong University of Technology. His research interests include dynamic approaches for satellite-based gravity field determination, combined inversion derived from LEO satellite observations, and application of time-varying gravity field models.